

Special Issue: Mitochondria - From Diagnosis to Treatment

Review

Visualizing Mitochondrial Form and Function within the Cell

Brian Glancy^{1,2,*}

The specific cellular role of mitochondria is influenced by the surrounding environment because effective mitochondrial function requires the delivery of inputs (e.g., oxygen) and export of products (e.g., signaling molecules) to and from other cellular components, respectively. Recent technological developments in mitochondrial imaging have led to a more precise and comprehensive understanding of the spatial relationships governing the function of this complex organelle, opening a new era of mitochondrial research. Here, I highlight current imaging approaches for visualizing mitochondrial form and function within complex cellular environments. Increasing clarity of mitochondrial behavior within cells will continue to lend mechanistic insights into the role of mitochondria under normal and pathological conditions and point to spatially regulated processes that can be targeted to improve cellular function.

Mitochondria Function as Part of the Cellular Team

In recent years, it has become increasingly clear that all mitochondria are not the same. Indeed, mitochondrial form, mitochondrial protein and lipid composition (see [Glossary](#)), and mitochondrial function are all now known to vary according to the type of cells in which they reside [1–7] because mitochondrial function within a given cell appears to be tuned to help achieve the overall functional goals of that particular cell. In other words, mitochondria are team players and adapt to fit the needs of the team. Regardless of whether its major output is ATP, signaling molecules, or other metabolites, how well a mitochondrion is able to perform its required functions within a cell is intrinsically dependent on its spatial relationships with other components within or nearby that cell ([Figure 1](#)).

With the aim of better understanding how mitochondria support cellular functions and how this support may be altered by disease states, biologists have begun to use a variety of innovative imaging techniques to visualize mitochondrial structure and function within the context of the rest of the cell. Here, I discuss the ins and outs of recent advances in mitochondrial imaging that are generating new hypotheses and contributing mechanistic insights into the relationships between mitochondrial form and function within cells.

Mitochondrial Form

The structure of mitochondria within a cell, together with mitochondrial protein and lipid composition, dictates the capacity for mitochondrial function within that cell (see Clinician's Corner). Cellular conditions at any given time will determine how much of that capacity will be used in that moment, but maximal mitochondrial function will always be limited by: (i) the amount of mitochondria within a cell; (ii) the internal components within mitochondria; and (iii) the ability of mitochondria to interact with other cellular structures to receive inputs and deliver products as needed. While biochemical methods [8,9] or protein analyses [10–12] can be used to assess some of the parameters involved in determining mitochondrial functional capacity, microscopic observations of mitochondria can be used to evaluate each aspect within the spatial context of the intact cell. The two primary types of microscopy used for viewing mitochondrial form within cells are light microscopy and electron microscopy ([Figure 2](#)), and each hold specific advantages for measuring different structural characteristics ([Table 1](#)). Below I discuss recent breakthroughs as well as examine the benefits and tradeoffs associated with currently available options for visualizing mitochondrial structure.

Highlights

Advances in super-resolution microscopy now enable the visualization of thousands of individual mitochondria with molecular precision throughout large tissues, as well as unprecedented views of the dynamic nature of internal mitochondrial structures.

Expansion of our ability to simultaneously visualize multiple mitochondrial structures and proteins together with other organelles has provided novel mechanistic insights into the intra- and inter-organelle interactions of mitochondrial networks.

Spatially resolved measures of mitochondrial energetic flux provide a promising avenue for evaluating the impact of interventions into cellular energy metabolism within heterogeneous cells and tissues.

Accompaniment of high-throughput image analysis platforms with big data-generating microscopy approaches now enables systems-level evaluations of how mitochondria behave within the cellular environment.

¹National Heart, Lung, and Blood Institute, National Institutes of Health, Bethesda, MD, USA

²National Institute of Arthritis and Musculoskeletal and Skin Diseases, National Institutes of Health, Bethesda, MD, USA

*Correspondence: brian.glancy@nih.gov



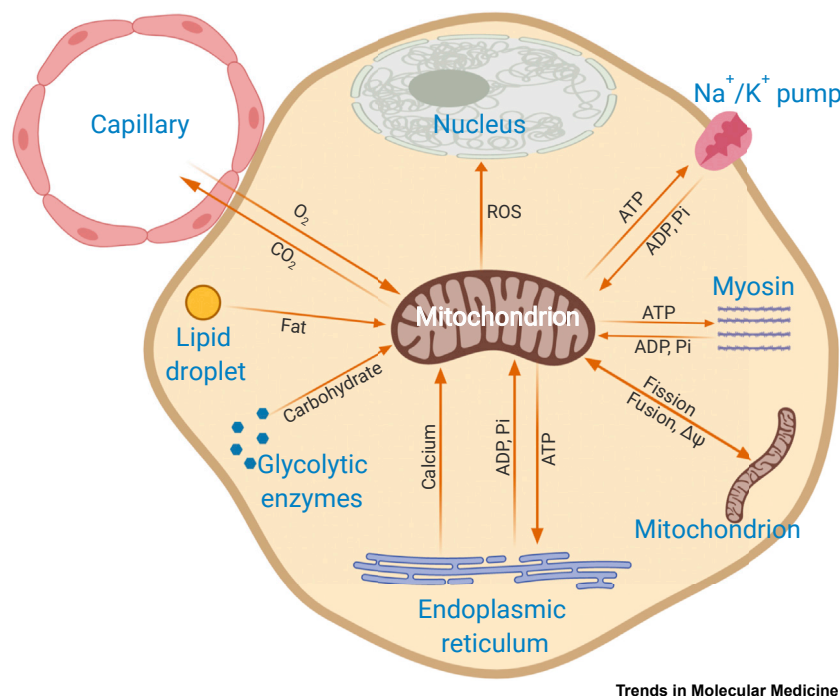


Figure 1. Mitochondrial Function Relies on Cellular Interactions.

Depiction of a mitochondrion within a cell highlighting some of the many interactions with other cellular structures that can regulate acute mitochondrial function. Mitochondrial inputs are listed next to arrows pointing toward the mitochondrion, and mitochondrial products are listed next to arrows pointing away from the mitochondrion. Interactions involved in assembling and degrading mitochondria are not shown. Structures not drawn to scale.

Mitochondrial Content

The number of mitochondria within a cell, or mitochondrial content, is generally considered to be proportional to cellular capacity for mitochondrial function. While there are several methods for measuring cellular mitochondrial content [2,13–17], imaging is the only way to directly assess the volume of a cell that is occupied by mitochondria. For light microscopy, there are three general approaches to visualizing mitochondrial structures: (i) labeling mitochondria in live cells with fluorescent dyes; (ii) immunostaining **fixed cells** with mitochondria-specific fluorescent antibodies; and (iii) using genetically encoded fluorescent mitochondrial tags. Using live cell fluorescent dyes to assess mitochondrial structure is straightforward in theory because all it takes is incubating the cells of interest with the dye for 20–60 min and then imaging and analyzing cellular fluorescence. The MitoTracker (MT) series of dyes are commonly used to assess mitochondrial content and work by binding to thiol groups within the mitochondria [18]. MT Orange, Red, and Far-Red dyes all load into the mitochondria according to the mitochondrial membrane potential ($\Delta\Psi$); thus, differences in mitochondrial fluorescence between cells may be attributable to altered cellular conditions rather than to a difference in mitochondrial content. MT Green is considered to load independent of $\Delta\Psi$ and, thus, is a more consistent marker of content for most live cells. However, MT Green is not retained well in cells after fixation and, therefore, the other MT dyes may become a better option, for example, when combining MT with antibody labeling of specific proteins or when using fixation to stop cellular or mitochondrial movement while imaging. Additionally, MT Green was recently shown to be sent out of mitochondria by xenobiotic efflux pumps in hematopoietic stem cells [13]. This information, combined with the known toxicity of mitochondrial dyes [19], suggests that, while fluorescent dyes can be used to assess mitochondrial content quickly, results should be interpreted with appropriate caution.

Similar in concept to a spatially resolved western blot, immunofluorescent staining can simultaneously be performed on multiple mitochondrial or other cellular proteins to assess structure and

Glossary

Capacity for mitochondrial function: maximal function of mitochondria possible. The capacity for mitochondrial function within a cell is determined by mitochondrial structure, composition, and interactions with other structures.

Electron microscopy: microscopy technique using electron beams to illuminate and magnify structures. Electron microscopy can resolve much smaller structures than light microscopy. Grayscale images are generated, where the contrast depends on the electron density of cellular structures.

Many structures can be visualized simultaneously. Metallic stains can be used to increase contrast in specific structures.

Fixed cells: cells that have been preserved from biological decay. Several methods of fixation are commonly used, such as rapid freezing or chemical fixation by formaldehyde or methanol.

Fluorophore: fluorescent molecule that emits light when excited by a light beam. Fluorophores come in many varieties, including the color of light needed for excitation as well as the color emitted after excitation.

Immunogold: method for antibody labeling of specific proteins in electron microscopy. Instead of using a fluorescently tagged secondary antibody as with light microscopy, the secondary antibody is conjugated with tiny gold particles, which appear as electron-dense dots in an electron microscopy image.

Light microscopy: microscopy technique using visible light beams to illuminate and magnify structures. For mitochondria, this generally involves excitation of fluorescent molecules and detection of the resultant emitted light.

Mitochondrial protein and lipid composition: proteins and lipids that comprise a mitochondrion. Proteins can be used to transport molecules, catalyze molecular reactions, and build or break down structures among other things.

Lipids provide structural support to membranes and some can be synthesized within mitochondria.

Super-resolution: specific type of light microscopy where the achievable resolution is better than the diffraction limit of light

content within fixed cells in a process that takes 1–2 days. Antibodies are generally available from several sources and can often be used with a **fluorophore** of choice, leading to great experimental flexibility. The choice of antibody should be for mitochondrial proteins the expression level of which per mitochondrion is not expected to be altered between comparison groups to separate changes in mitochondrial content from changes in mitochondrial composition. Also, targeting more abundant mitochondrial proteins [e.g., voltage-dependent anion channel (VDAC)] should result in stronger antibody labeling, brighter fluorescence, and, thus, easier image analysis and interpretation. One downside of immunofluorescence is potential nonspecific antibody labeling of untargeted proteins, which can confound structural assessments; therefore, using validated antibodies or performing control experiments is recommended. Additionally, uniform antibody penetration throughout thick cells or tissues has traditionally been a problem, but recently developed tissue-clearing techniques, such as CLARITY, SWITCH, or iDISCO, can be used to overcome this issue [20–22].

(~200 nm). For over 100 years, the diffraction limit was thought to set the highest resolution achievable, until several recent developments broke through this barrier.

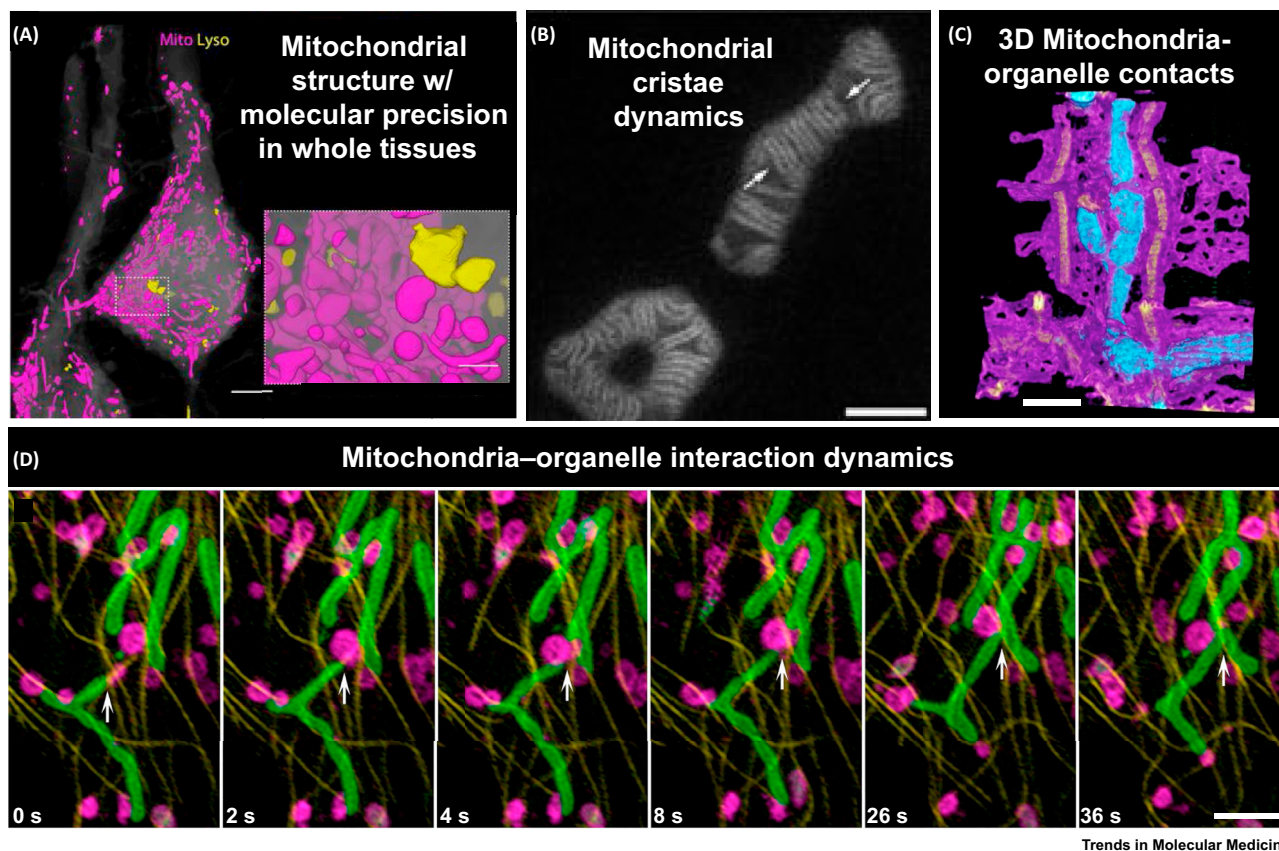
Genetically encoded fluorescent mitochondrial tags provide specific and stable labeling of mitochondrial structures within cells and can be targeted either to specific proteins or to the mitochondrial matrix in general using a mitochondrial-targeting sequence. Transgenic labeling is often the approach of choice for cell biologists due to the relative ease of transfection of cell lines, although transfection efficiency is often lower in primary cell cultures and live animals. Compared with the abundance of antibodies, there are fewer transgenic constructs available to label mitochondria. Additionally, genetically encoded cell cultures and animals can take days to months to develop, respectively, making time a major limitation of this approach.

Mitochondrial Shape

The approaches to visualizing mitochondrial shapes are similar to those described for mitochondrial content, although assessing individual mitochondrial shapes requires higher resolution images. In many cases, the maximum resolution allowed by traditional light microscopy (~200–250 nm in x,y, 500 nm in z) is insufficient to clearly resolve individual mitochondrial structures, necessitating the use of electron microscopy (maximum resolution ~0.2 nm). However, early in 2019, the Betzig and Boyden laboratories reported on a recent collaboration that overcame this resolution limitation and allowed for assessment of thousands of individual mitochondrial shapes with molecular precision in whole tissues [23]. They combined expansion microscopy (ExM) with lattice light sheet microscopy (LLSM), each recent major breakthroughs for imaging cellular structures [24,25]. ExM, which achieves **super-resolution** by physically magnifying biological samples rather than optical magnification and, thus, can be performed with any light microscope, involves embedding fixed samples labeled with either antibodies or transgenic fluorophores in a swellable polymer gel, digestion of unlabeled tissue, and then expanding the gel in a solvent. ExM has been used to increase resolution up to 20-fold [26], but a fourfold increase may be a more realistic goal for uniform expansion without distortion of cellular structures [23]. A disadvantage of ExM is that image acquisition times and file sizes increase proportionally to the level of expansion cubed for 3D data (i.e., 4× expansion → 64-fold more data). LLSM together with ExM overcomes the speed issue by sweeping a thin sheet of Bessel beams through the sample perpendicular to the objective, with the resulting fluorescence collected by a high-speed camera at rates of several hundred images per second and with little photobleaching. This combined approach will be useful for future studies evaluating mitochondrial structure in whole tissues or large cells, such as cardiac and skeletal muscle or neurons, although the fixation required for ExM does not permit the study of live cells.

Mitochondrial Ultrastructure

The mitochondrial inner membrane contains many folds called cristae, which can regulate the organization, and, thus, function of the enzymes involved in energy conversion and reactive oxygen species (ROS) production [27–29]. Also contained within mitochondria are nucleoids, which enclose mitochondrial DNA (mtDNA). Due to the small sizes of the internal mitochondrial components and spaces (~100 nm or less), visualization of mitochondrial ultrastructure has typically been performed using electron microscopy on fixed cells [30–32]. However, the emergence of, and continued improvements, in super-resolution light microscopy have opened a window into mitochondrial ultrastructure within live cells. Super-resolution (stimulated emission depletion; STED) microscopy was recently used to visualize individual ellipsoid-shaped



Trends in Molecular Medicine

Figure 2. Recent Advances in Mitochondrial Imaging.

(A) Fluorescent antibody-labeled mitochondria (magenta) and lysosomes (yellow) within two layer V pyramidal neurons of the mouse somatosensory cortex visualized by expansion lattice light sheet microscopy. Scale bars: 5 μm (inset 1 μm). Reproduced, with permission, from [23]. (B) Mitochondrial cristae structure within live HeLa cells expressing a Cox8a-SNAP fusion protein and labeled with SNAP-Cell SiR dye as imaged by a stimulated emission depletion super-resolution microscope. Arrows highlight cristae voids occupied by mitochondrial nucleoids. Scale bar: 1 μm . Reproduced, with permission, from [36]. (C) 3D rendering of contacts between mouse skeletal muscle mitochondria (cyan), sarcoplasmic reticulum (magenta), and t-tubules (orange), visualized with focused ion beam scanning electron microscopy and machine-learning organelle segmentation. Scale bar: 1 μm . Reproduced, with permission, from [2]. (D) Dynamic interactions between genetically encoded mitochondria (mEmerald-Tomm20, green), lysosomes (HaloTag-Lamp1, magenta), and microtubules (mCherry-ensconsin, yellow) in COS-7 cells visualized on a grazing incidence structured illumination microscope. Arrows indicate a mitochondrion hitchhiking on a lysosome prior to fusion. Scale bar: 1 μm . Reproduced, with permission, from [40].

mtDNA nucleoids, finding that each nucleoid contains a single copy of mtDNA that is compacted by mitochondrial transcription factor A (TFAM) [33]. STED microscopy works by using a second laser to selectively deplete the emission of a fluorophore, with the shape of the additional laser resembling a donut. Thus, the remaining nondepleted fluorescence is in the shape of the donut hole, or smaller ($\sim 30\text{--}80\text{ nm}$ resolution) than that achieved without using the depletion laser. STED can be used in tandem with confocal microscopy and is even available as a modular add-on in some commercial systems. This can be useful when imaging multiple fluorophores that do not all require super-resolution (e.g., nuclei or lipid droplets) because the depletion laser can be selectively used for some or none of the fluorophores and reduces the potential photodamage from additional laser exposure.

The shape of mitochondrial cristae and how the structures change across time have also been traditionally difficult to capture in live cells [34,35]. Recently, a STED approach to imaging cristae was developed using a genetically encoded mitochondrial inner membrane SNAP-tag, which could then be linked with a fluorophore of choice, allowing simultaneous visualization of cristae and mtDNA nucleoids with $\sim 50\text{-nm}$ resolution [36]. However, photobleaching limited the time course of imaging

Table 1. How to Visualize Mitochondrial Form and Function

Mitochondrial parameter	Light microscopy	Electron microscopy
Content	Straightforward for detecting large changes in mitochondrial content. Super-resolution increases the sensitivity to detect smaller changes. Care must be taken that membrane potential or protein expression changes do not confound results if using dyes or antibodies, respectively.	High resolution permits detection of small differences in content. Must ensure that images adequately represent the entire cell volume. Segmentation of grayscale images can be more difficult than specifically labeled light microscopy images.
Shape	Easily used to compare elongated and spherical mitochondrial shapes. May lack resolution to discriminate between individual mitochondrial structures.	Individual mitochondria are easily observed and measured. 2D images may be misleading due to inability to see complete 3D structure.
Ultrastructure	Recommended for mtDNA nucleoids, which can be labeled transgenically with antibodies or dyes. Super-resolution microscopy is approaching capacity to resolve inner membrane and matrix spaces.	Recommended for cristae junctions, inner membrane, and matrix spaces due to higher resolution. Often difficult to see mtDNA nucleoids.
Protein localization	Recommended due to ease of specific antibody or transgenic labeling of proteins.	Further developments are needed. Current transgenic approaches have proven difficult to adapt across models, particularly in animals. Immunogold is easier but lacks precision.
Organelle interactions	Recommended for observing dynamic organelle interactions due to availability of transgenic and dye labeling approaches for multiple structures in live cells. Generally lacks resolution to specifically detect functional contacts (<30 nm) between organelles. The number of organelle types observed can be limited by ability to specifically label different structures.	3D approaches are ideal for assessing direct organelle interactions due to high resolution and ability to discern up to ten or more structures per cell volume. Accurate and fast image segmentation of grayscale image volumes is current limitation. 2D images are informative, but lack complete picture of 3D images.
Energetics	Several dyes and endogenous markers are available to assess mitochondrial energetic status. Care should be taken that changes in fluorescence are not simply due to differences in mitochondrial content. Membrane potential probes may also be sensitive to changes in pH or ROS.	Not directly assessed by electron microscopy in cells.
Signaling	Several dyes and endogenous markers are available to assess mitochondrial calcium, ROS, and redox status, among others. Care should be taken that changes in fluorescence are not simply due to differences in mitochondrial content. ROS and calcium probes may be sensitive to changes in pH or membrane potential.	Not directly assessed by electron microscopy in cells.

(Continued on next page)

Table 1. Continued

Mitochondrial parameter	Light microscopy	Electron microscopy
Dynamics	Recommended for assessing frequency of fission and fusion events as well as motility due to ability to visualize live cells across time.	Mitochondria fixed during fission and fusion events can be observed, but unable to see live events.
Turnover	Several recently developed transgenic approaches are available for live cell assessment of mitophagy. Antibodies are also available for assessing mitophagy markers in fixed cells.	Mitochondria engulfed by autophagosomes or within lysosomes can be observed but can sometimes be difficult to discriminate from other structures. Cannot observe live events.

to 10–20 frames over 2 min. Development of another super-resolution microscopy approach (Hessian structured illumination microscopy; Hessian-SIM), which utilizes a grid illumination pattern together with a Hessian deconvolution algorithm to reconstruct high-resolution images at low light doses, allowed visualization of individual cristae with ~90-nm resolution for up to 800 frames using MT Green dye [37]. Thus, although STED approaches currently offer higher resolution, which may be important for mitochondria with tightly packed cristae, such as in the heart, SIM can be used to image faster and with less photobleaching and may be better for cells with highly dynamic mitochondria. Application of these and similar types of live cell imaging techniques [38–40] to specific biological questions will likely offer powerful insights into the dynamics of mitochondrial ultrastructure and potential functional roles during normal and pathological conditions.

Mitochondrial Protein Localization

Approaches for imaging mitochondrial or potential mitochondrial proteins are similar to those for other cellular structures and can be done with either antibodies or transgenic probes, as discussed earlier. Importantly, images should be taken at a high enough resolution to clearly discriminate between mitochondria and other closely associated organelles, such as the endoplasmic reticulum (ER) [41,42]. Determining which mitochondrial compartment or membrane a protein resides in can indicate the types of other protein it may interact with and offer further insights into potential protein function (Box 1). Super-resolution techniques, as discussed earlier, can provide enough resolution to discriminate between mitochondrial compartments in some cases [43,44]. Fluorescence lifetime imaging (FLIM) has also been used to distinguish between different mitochondrial compartments for genetically encoded proteins based on the length (lifetime) of exponential fluorescence decay after excitation using time-correlated single photon counting [45]. One advantage of FLIM is that several different proteins or molecules with the same or similar fluorescence emission wavelengths can be differentiated if the lifetimes can be clearly resolved [46].

Mitochondrial protein localization can also be assessed by performing **immunogold** labeling, which is similar to immunofluorescence labeling, but instead of a fluorophore, the secondary antibody is labeled with 5–10-nm gold particles that appear as electron-dense spots in electron microscopy images [47,48]. Analysis of immunogold-labeled images relies on labeling density near the structure of interest and can be confounded by background signal from nonspecific antibody labeling. Recently, genetically encoded tags for electron microscopy were developed (e.g., miniSOG and APEX) [49–52], which can be linked to a protein of interest to provide increased image contrast where the protein resides within mitochondria or the cell. miniSOG relies on exposing an internal flavoprotein to UV light, resulting in the generation of singlet oxygen, which then polymerizes added diaminobenzidine (DAB), leading to an increase in electron density after addition of osmium. APEX works similarly but is a modified ascorbate peroxidase that polymerizes DAB upon exposure to hydrogen peroxide. Use of miniSOG and APEX requires careful titration of the UV dose and hydrogen peroxide exposure, respectively, to polymerize enough DAB to increase electron density but not too much that the

Box 1. Tandem Labeling Approaches for Evaluating Submitochondrial Protein Localization

Visualizing the intramitochondrial localization of proteins without the use of specialized super-resolution or FLIM equipment can be done using one of several tandem labeling approaches. The split fluorophore (e.g., split-GFP) approach involves genetically labeling the protein of interest with half of a fluorophore and a potential interacting protein with the other half, resulting in fluorescence only where the two proteins are in close enough proximity (~10–50 nm depending on the length of spacer encoded on one end [111]) to combine into the complete fluorophore [112,113].

FRET relies on genetically encoding one protein with a donor fluorophore and the other with an acceptor fluorophore [114,115]. When the two proteins are in close proximity, the FRET donor transfers energy to the acceptor, resulting in increased fluorescence of the acceptor and a decrease in that of the donor. Thus, the fluorescence ratio of the two fluorophores is the measured output for FRET. Only specific fluorophore pairs work with FRET (e.g., YFP+CFP) and the use of two fluorophores takes up more of the emission bandwidth than the split-GFP approach; however, because the energy transfer efficiency is directly related to the distance between fluorophores, FRET can be used to more quantitatively assess the distance between proteins.

Proximity ligation assays (PLA) [116] label both proteins with primary antibodies and secondary antibodies linked to specific short DNA strands, such that, when the two proteins are in proximity, the two DNA strands form a circular DNA molecule, which can be amplified and bound by fluorescently labeled oligonucleotides, resulting in fluorescence specific to the sites of protein interaction. PLA does not require transgenic expression of probes and, thus, is more readily available across model systems compared with the split-GFP or FRET approaches. However, PLA also requires fixation and, therefore, cannot be used to monitor dynamic events in live cells.

increased electron density spreads beyond the protein of interest. Compared with the adoption of fluorescently tagged proteins a decade ago, application of genetically encoded electron microscopy tags has moved more slowly, perhaps due to the sensitivity of the DAB polymerization step or the inherently slower nature of electron versus light microscopy. At current rates, pushing the boundaries of super-resolution light microscopy appears to be the more promising avenue to pursue for high-resolution assessment of mitochondrial protein localization.

Mitochondria–Organelle Interactions

Simultaneous imaging of multiple organelles is a powerful tool for assessing how the components of a cell, including mitochondria, work together to achieve functional goals. A few years ago, a novel multispectral imaging approach was developed that allowed the simultaneous visualization of six different organelles, including mitochondria, across time and in 3D to show that the dynamic organelle interactome was dependent on a functional microtubule system in COS-7 cells [53]. Cells were excited sequentially by six different lasers, emitted light was collected through a series of interference filters, and then a spectral unmixing algorithm was applied to every pixel to separate the cyan fluorescent protein (CFP), enhanced (E)GFP, yellow (Y)FP, mApple, Texas Red, and Bodipy fluorescent signals corresponding to different organelles. While this multispectral imaging technique can be applied to any cellular structures on any light microscope in theory, the authors used confocal and light sheet microscopes where the resolution achieved (>300 nm) was insufficient to evaluate the specialized functional contacts that occur between organelles when they were within 30 nm of each other [54]. Application of multispectral imaging to super-resolution microscopes capable of resolving functional contacts between mitochondria and other organelles would provide a powerful tool for systems-level evaluation of dynamic organelle interactions within the cell.

Bleck *et al.* [2] were able to bypass the resolution limits of light microscopy by using 3D electron microscopy (focused ion beam scanning electron microscopy; FIB-SEM) combined with machine-learning image segmentation to show that the intra- and interorganelle interactions within muscle mitochondrial networks are altered in accordance with the functional goals of different muscle cell types. FIB-SEM images the surface of a fixed sample and then uses an ion beam to remove the top layer of the sample, repeating this process many times. Analysis of the resultant 3D volume of

hundreds or thousands of grayscale images can be a major limitation of this technique due to the time required to segment different cellular structures [55,56]. Machine-learning techniques in which several training images are used to classify which pixels correspond to mitochondria or other cellular structures and then applied over the entire volume can speed up image segmentation by several thousand-fold with high accuracy [57,58]. In addition to higher resolution, expression of transgenic probes or use of fluorescent dyes is unnecessary to discriminate between mitochondria, ER, or many other cellular structures with electron microscopy because they can be specified by their characteristic structure in any fixed cell, although the visibility and contrast of different cellular structures is dependent on the heavy metal and other stains used (e.g., osmium, tannic acid, thiocarbazine, etc.). High-throughput analysis of functional organelle interactions throughout the cell provides a promising platform for dissecting how cellular structural design translates to cellular function or dysfunction.

Mitochondrial Function

One of the major issues of functional imaging is that, unlike structural imaging where a single snapshot is often sufficient, functional imaging generally requires the collection of many images in living cells or tissue across time. Since electron microscopy cannot be performed on living tissue (the electron beams completely destroy live cells) [59], light microscopy is the primary tool for visualizing mitochondrial function within cells. However, while less damaging than electron beams, shining light beams on cells can still cause damage either to the cells or the fluorophores being excited [60]. Thus, the more times a cell or region of a cell is imaged, the greater the likelihood of damage occurring. The issue of photodamage sets off a delicate balance, where attempts are made to shine a minimal amount of light on cells for the least amount of time while still shining enough light to get high **signal:noise ratios (SNRs)** and imaging often enough to adequately describe the functional events taking place [60]. This balancing act can vary greatly because the requirements for spatial and temporal resolution as well as signal:noise ratio differ for each biological question and can also be dictated by the sensitivity and intensity of the fluorophore(s) being imaged. Unfortunately, there is no one-size-fits-all approach to functional mitochondrial imaging. However, faster and gentler microscopes, as well as brighter and more stable fluorophores, continue to be developed, allowing for a clearer window into how mitochondria behave within cells. Here, I discuss these recent advances and the current state-of-the-art for functional mitochondrial imaging.

Mitochondrial Energetics

One of the most important functions of mitochondria is to make ATP. Thus, it is of interest to visualize how well mitochondria perform this task within cells. Indeed, there are several dyes or genetically encoded probes of varying specificity that enable observation of ATP in cells [61–63]. One of these methods, ATeam [61], is a genetically encoded Förster resonance energy transfer (FRET) probe where, instead of putting the donor and acceptor fluorophores on two different proteins as discussed in [Box 1](#), the two fluorophores are linked by a protein that changes conformation upon ATP binding, thus bringing the two fluorophores close enough to induce FRET. ATeam is insensitive to pH and can be targeted to either the cytosol or mitochondria, making it useful for assessing pathological changes in cellular energy metabolism [64].

Approaches to imaging other components of the mitochondrial energy conversion pathway include observing mitochondrial pyruvate, redox status, and $\Delta\Psi$ [65–67] ([Boxes 2 and 3](#)). While each of these approaches provides information on the concentration of energetic markers, the concentration of each reflects the balance between its production and utilization within the cell. As a result, if production continues to match utilization during an increase in energy demand, a common occurrence in cells [68–70], concentration of the energetic marker will not indicate that the energetic environment in the cell is different. The ideal marker of mitochondrial energetic function would be a direct measure of how fast mitochondria are making ATP. Unfortunately, a robust, spatially resolved measure of the rate of ATP production is not currently available. Oxygen consumption is proportional to ATP production, but while methods to image oxygen within cells are improving, current developments have primarily focused on visualizing oxygen content rather than on the rate of oxygen consumption [71,72].

Box 2. Assessing Mitochondrial NADH Redox Status

The redox status of the mitochondrial NADH pool can be assessed through its endogenous autofluorescence [65,117] because the NADH molecule itself fluoresces, meaning there is no need for additional probes. However, NADH autofluorescence requires UV (~340–375 nm) excitation, which is not available with most commercial confocal microscope systems, requiring the use of more expensive two-photon lasers to excite NADH with higher (double) wavelength (~680–750 nm) pulses. Additionally, NADH and another redox molecule, NADPH, have identical optical properties, making it difficult to evaluate them separately when present in similar quantities [46], although FLIM offers one approach [46]. For these reasons, transgenic NADH probes have been developed using cpYFP linked to a Rex homodimer (Fret-Mit), both of which change conformation upon NADH binding, leading to increased fluorescence proportional to NADH concentration [118]. The cpYFP approach is reported to result in a greater fluorescent dynamic range compared with FRET probes [119]; however, the fluorescent intensity of Fret-Mit is sensitive to both NADH and pH, limiting its usefulness to questions where pH can be controlled for. Targeting pH-resistant, cytosolic NADH probes, such as SoNar [120], to the mitochondria in a cell-specific manner (e.g., conditional expression through Cre recombinase) would be helpful for evaluating the redox status of small cells with low mitochondrial content (i.e., low endogenous NADH fluorescence) within large tissues, such as endothelial or satellite cells within skeletal muscle.

An initial approach to provide a spatially resolvable measure of the rate of mitochondrial energy conversion was recently published [73], where monitoring of the kinetic response of endogenous mitochondrial NADH fluorescence (Box 2) to rapid inhibition of NADH utilization allowed the rate of NADH production to be measured in live mouse skeletal muscle and in cultured neurons under a multiphoton microscope. Further development of methods to quantify rates of mitochondrial ATP production or proportional measures (e.g., oxygen or NADH) would allow improved testing of how pharmacological interventions affect mitochondria within different regions of the same cell or tissue.

Mitochondrial Signaling

The most well-described mitochondrial signaling molecules are cytochrome c, calcium, ROS, and the redox pairs discussed earlier (NAD^+/NADH and $\text{NADP}^+/\text{NADPH}$). Several cytochrome c probes have recently been synthesized with the aim of better understanding apoptosis [74–82]; however, to date, they have been little used to answer specific questions. Future application of these probes to biological questions will be needed to determine the advantages and disadvantages of each for specific

Box 3. Mitochondrial Membrane Potential Probes

There are several commonly used $\Delta\Psi$ -sensitive dyes (TMRM, TMRE, Rhod123, and JC-1), which are all lipophilic cations and accumulate proportionally to the voltage across membranes. Given that these dyes accumulate across both the cell membrane and the mitochondrial inner membrane, measures of total cellular fluorescence or only mitochondrial fluorescence can be affected by changes in the plasma membrane potential [121]. Thus, imaging at sufficient resolution to measure the mitochondrial-to-cytosolic fluorescence ratio allows evaluation of $\Delta\Psi$ -independent of changes in plasma membrane voltage. TMRM, TMRE, and Rhod123 each contain one fluorophore, whereas JC-1 fluorescence shifts from green to red with increasing aggregation in the matrix and, thus, is used ratiometrically. However, there are many reported problems with JC-1, including insensitivity to small voltage changes, high photosensitivity, slow equilibration times across membranes, and being prone to artifacts [19], suggesting that it should be used with caution, if at all. TMRM and TMRE equilibrate more quickly (~15 min) than Rhod123, and TMRE and Rhod123 are more toxic than TMRM [19]. Additionally, use of probes above ~100 nM can initiate ‘quench mode’, where the concentration of the probe is so high inside the mitochondria that aggregated dye quenches emitted fluorescence resulting in an increased signal when $\Delta\Psi$ decreases (less quenching) and a decreased signal when $\Delta\Psi$ increases (more quenching). Thus, using the lowest possible concentration of these probes is recommended. Proper imaging of $\Delta\Psi$ can then be multiplexed with cellular (e.g., calcein-AM) and nuclear (e.g., Hoechst) dyes for high-throughput analysis of mitochondrial structure and function within dynamic cell populations under normal or pathological conditions [15].

Clinician’s Corner

- The function of mitochondria within a cell is regulated by the number of mitochondria within the cell, their composition, and how well they are able to communicate with other organelles. A better understanding is needed of how each aspect of mitochondrial function contributes to overall cellular function in both health and disease.
- Dysfunctional mitochondria are the cause for a heterogeneous group of devastating human disorders referred to as ‘Mitochondrial Diseases’, for which no cure currently exists. Novel imaging approaches may help further understand the underlying pathologies.
- Mitochondrial structures within cells can be visualized to provide an index of capacity for mitochondrial function. Recent developments in microscopy now allow simultaneous imaging of multiple proteins or molecular targets within mitochondria and how they interact with other cellular structures.
- Measurement of mitochondrial structure, together with function within the context of the entire cell may help facilitate the identification and/or impact of potential therapeutic targets aimed at improving cellular function.
- Application of antibody and fluorescent dye-based techniques are well suited for visual evaluation of mitochondrial form and function in patient blood samples and tissue biopsies using relatively few cells compared with biochemical or molecular biology approaches. Genetically encoded indicators of mitochondrial structure and function provide an additional suite of tools compatible with patient-derived cell lines.

experimental models. Sensors are available in many forms and have been well characterized and discussed extensively elsewhere for both calcium [83–91] and ROS [92–95], and can also be multiplexed with other measures of mitochondrial structure and function [96].

In addition to signaling with other organelles, mitochondria have also been reported to communicate among themselves through intermitochondrial junctions or mitochondrial nanotunnels [97–100]. While conduction of $\Delta\Psi$ among connected mitochondria has been assessed by comparing the tetramethyl rhodamine, methyl ester (TMRM) response of mitochondria adjacent to a region of photoactivatable depolarization [2,97,101], propagation of the chemical component of the protonmotive force across the inner mitochondrial membrane, ΔpH , between adjacent mitochondria has also been shown by the Demaurex group [102]. Mitochondrial pH can be visualized ratiometrically with a genetically encoded, pH-sensitive circularly permuted (cp)YFP (MitoSypHer) [103], which is a mutation of the ROS probe, Hyper [104], to remove the sensitivity to hydrogen peroxide. By combining MitoSypHer with a photoactivatable mitochondrial matrix GFP (paGFP), Santo-Domingo *et al.* [102] showed that rapid electrical coupling could occur between adjacent mitochondria without exchange of matrix contents (i.e., paGFP), and demonstrated the applicability of using multiple mitochondrially targeted probes to elucidate mechanistic information about the nature of ion versus protein exchange between adjacent mitochondria.

Mitochondrial Dynamics and Turnover

Another major function that mitochondria are tasked with is to contribute to their own self-maintenance. The removal of damaged mitochondria through mitophagy can now be easily imaged thanks to the development of two recent genetically encoded probes (mt-Keima and mito-QC) [105–107]. Mitochondrial matrix-targeted mt-Keima utilizes a ratiometric, dual excitation system in which excitation with 458-nm light illuminates mitochondria with a neutral or slightly alkaline pH and 561-nm light excites mitochondria in the acidic environment of the lysosome. Mito-QC comprises two fluorophores, GFP and mCherry, linked to the outer mitochondrial membrane protein Fis1, and detects mitophagy by the loss of GFP signal in the acidic lysosome. While both probes are compatible with live cell imaging, mt-Keima cannot be used in fixed cells, precluding its use in tandem with immunofluorescent staining of other proteins. However, the large emission bandwidth used by mito-QC also limits its compatibility with additional indicators to either blue or far-red-emitting probes.

Maintenance of high-quality mitochondria also involves the proper replication and transmission of mtDNA. It is well known that an exchange of mitochondrial contents can occur when mitochondria undergo fission and fusion [108–110]. However, until recently, it was unknown how or whether this process involved mtDNA. Lewis *et al.* [42] used three transgenic fluorophores targeted at the same time to the mitochondrial matrix [blue fluorescent protein (BFP)], mtDNA nucleoids (GFP), and ER (mCherry) to show that replicating mtDNA nucleoids mark the sites of mitochondrial fission, which is then mediated by the ER. Thus, simultaneous imaging of two mitochondrial structures and the ER revealed a mechanism of how alterations in mitochondrial shape and ultrastructure can be regulated in coordination with specific interactions between organelles, further highlighting the integrated nature of cellular processes and the role of mitochondria within them.

Concluding Remarks

The emergence of mitochondria as multifaceted organelles tailored to support cellular function has helped drive the development of new imaging approaches aimed at better understanding the mechanisms that guide mitochondrial function within complex cellular environments. Continued improvements in light microscopy, particularly super-resolution microscopy, offer a promising path toward visualizing mitochondrial behavior with molecular precision, while increasing accessibility to 3D electron microscopy techniques is expanding our knowledge of how mitochondria interact with other organelles to meet cellular objectives. There remains an unwavering goal to image faster, gentler, with higher resolution, across larger volumes, and a greater number of molecules or structures, which continues to guide technological development (see Outstanding Questions). As approaches to imaging mitochondria as part of complex cell systems are realized, the development of big data analytical

Outstanding Questions

Can super-resolution microscopy meet or surpass the resolution of large-scale, 3D electron microscopy techniques?

Can methods for genetically encoding tags in electron microscopy be improved to facilitate widespread use, akin to that of genetically encoded fluorescent tags?

How can the number of mitochondrial proteins or molecules that can be imaged simultaneously by the light microscope be increased? Will multispectral or fluorescent lifetime imaging lead the way?

Can spatially resolved measures of mitochondrial function reach the quantitative rigor of biochemical methods?

Will a widely accepted, quantitative measure describing the large variety of mitochondrial shapes be developed?

Is the frequency of dynamic mitochondrial cristae events proportional to the frequency of mitochondrial fission and fusion events?

What will it take to measure ATP production rates with subcellular resolution?

Can current and future advancements in cellular imaging be applied to tissues in live animals and humans?

As imaging speed, resolution, volume, and the number of structures imaged all increase, how do we analyze and interpret the very large data sets that will be generated?

platforms will be necessary to fully elucidate the principles that govern mitochondrial form and function across health and disease.

References

- Benador, I.Y. et al. (2018) Mitochondria bound to lipid droplets have unique bioenergetics, composition, and dynamics that support lipid droplet expansion. *Cell Metab.* 27, 869–885
- Bleck, C.K.E. et al. (2018) Subcellular connectomic analyses of energy networks in striated muscle. *Nat. Commun.* 9, 5111
- Johnson, D.T. et al. (2007) Functional consequences of mitochondrial proteome heterogeneity. *Am. J. Physiol. Cell Physiol.* 292, C698–C707
- Kim, Y. et al. (2019) Protein composition of the muscle mitochondrial reticulum during postnatal development. *J. Physiol.* 597, 2707–2727
- Porat-Shliom, N. et al. (2019) Mitochondrial populations exhibit differential dynamic responses to increased energy demand during exocytosis in vivo. *iScience* 11, 440–449
- Vega, R.B. and Kelly, D.P. (2017) Cardiac nuclear receptors: architects of mitochondrial structure and function. *J. Clin. Invest.* 127, 1155–1164
- Fecher, C. et al. (2019) Cell-type-specific profiling of brain mitochondria reveals functional and molecular diversity. *Nat. Neurosci.* 22, 1731–1742
- Zhang, H. et al. (2016) NAD(+) repletion improves mitochondrial and stem cell function and enhances life span in mice. *Science* 352, 1436–1443
- Kaufmann, U. et al. (2019) Calcium signaling controls pathogenic Th17 cell-mediated inflammation by regulating mitochondrial function. *Cell Metab.* 29, 1104–1118
- Weidberg, H. and Amon, A. (2018) MitoCPR—A surveillance pathway that protects mitochondria in response to protein import stress. *Science* 360, eaan4146
- Richter-Dennerlein, R. et al. (2016) Mitochondrial protein synthesis adapts to influx of nuclear-encoded protein. *Cell* 167, 471–483
- Gray, M.W. (2015) Mosaic nature of the mitochondrial proteome: Implications for the origin and evolution of mitochondria. *Proc. Natl. Acad. Sci. U S A* 112, 10133–10138
- de Almeida, M.J. et al. (2017) Dye-independent methods reveal elevated mitochondrial mass in hematopoietic stem cells. *Cell Stem Cell* 21, 725–729
- Wu, Z. et al. (1999) Mechanisms controlling mitochondrial biogenesis and respiration through the thermogenic coactivator PGC-1. *Cell* 98, 115–124
- Iannetti, E.F. et al. (2016) Multiplexed high-content analysis of mitochondrial morphofunction using live-cell microscopy. *Nat. Protoc.* 11, 1693–1710
- Wredenberg, A. et al. (2002) Increased mitochondrial mass in mitochondrial myopathy mice. *Proc. Natl. Acad. Sci. U S A* 99, 15066–15071
- Hansson, A. et al. (2004) A switch in metabolism precedes increased mitochondrial biogenesis in respiratory chain-deficient mouse hearts. *Proc. Natl. Acad. Sci. U S A* 101, 3136–3141
- Chazotte, B. (2011) Labeling mitochondria with MitoTracker dyes. *Cold Spring Harb. Protoc.* 2011, 990–992
- Perry, S.W. et al. (2011) Mitochondrial membrane potential probes and the proton gradient: a practical usage guide. *Biotechniques* 50, 98–115
- Murray, E. et al. (2015) Simple, scalable proteomic imaging for high-dimensional profiling of intact systems. *Cell* 163, 1500–1514
- Renier, N. et al. (2014) iDISCO: a simple, rapid method to immunolabel large tissue samples for volume imaging. *Cell* 159, 896–910
- Chung, K. et al. (2013) Structural and molecular interrogation of intact biological systems. *Nature* 497, 332
- Gao, R. et al. (2019) Cortical column and whole-brain imaging with molecular contrast and nanoscale resolution. *Science* 363, eaau8302
- Chen, F. et al. (2015) Optical imaging. Expansion microscopy. *Science* 347, 543–548
- Chen, B.C. et al. (2014) Lattice light-sheet microscopy: imaging molecules to embryos at high spatiotemporal resolution. *Science* 346, 1257998
- Chang, J.B. et al. (2017) Iterative expansion microscopy. *Nat. Methods* 14, 593
- Cogliati, S. et al. (2016) Mitochondrial cristae: where beauty meets functionality. *Trends Biochem. Sci.* 41, 261–273
- Quintana-Cabrera, R. et al. (2018) The cristae modulator Optic atrophy 1 requires mitochondrial ATP synthase oligomers to safeguard mitochondrial function. *Nat. Commun.* 9, 3399
- Friedman, J.R. et al. (2015) MICOS coordinates with respiratory complexes and lipids to establish mitochondrial inner membrane architecture. *Elife* 4, e07739
- Brandt, T. et al. (2017) Changes of mitochondrial ultrastructure and function during ageing in mice and *Drosophila*. *Elife* 6, e24662
- Scorrano, L. et al. (2002) A distinct pathway remodels mitochondrial cristae and mobilizes cytochrome c during apoptosis. *Dev. Cell* 2, 55–67
- Frey, T.G. and Mannella, C.A. (2000) The internal structure of mitochondria. *Trends Biochem. Sci.* 25, 319–324
- Kukat, C. et al. (2015) Cross-strand binding of TFAM to a single mtDNA molecule forms the mitochondrial nucleoid. *Proc. Natl. Acad. Sci. U S A* 112, 11288–11293
- Appelhans, T. et al. (2012) Nanoscale organization of mitochondrial microcompartments revealed by combining tracking and localization microscopy. *Nano Lett.* 12, 610–616
- Schmidt, R. et al. (2009) Mitochondrial cristae revealed with focused light. *Nano Lett.* 9, 2508–2510
- Stephan, T. et al. (2019) Live-cell STED nanoscopy of mitochondrial cristae. *Sci. Rep.* 9, 12419
- Huang, X. et al. (2018) Fast, long-term, super-resolution imaging with Hessian structured illumination microscopy. *Nat. Biotechnol.* 36, 451–459
- Shao, L. et al. (2011) Super-resolution 3D microscopy of live whole cells using structured illumination. *Nat. Methods* 8, 1044–1046
- Wang, C. et al. (2019) A photostable fluorescent marker for the superresolution live imaging of the dynamic structure of the mitochondrial cristae. *Proc. Natl. Acad. Sci. U S A* 116, 15817–15822
- Guo, Y. et al. (2018) Visualizing intracellular organelle and cytoskeletal interactions at nanoscale resolution on millisecond timescales. *Cell* 175, 1430–1442
- Phillips, M.J. and Voeltz, G.K. (2016) Structure and function of ER membrane contact sites with other organelles. *Nat. Rev. Mol. Cell Biol.* 17, 69–82

42. Lewis, S.C. et al. (2016) ER-mitochondria contacts couple mtDNA synthesis with mitochondrial division in human cells. *Science* 353, aaf5549
43. Stoldt, S. et al. (2019) Mic60 exhibits a coordinated clustered distribution along and across yeast and mammalian mitochondria. *Proc. Natl. Acad. Sci. U S A* 116, 9853–9858
44. Große, L. et al. (2016) Bax assembles into large ring-like structures remodeling the mitochondrial outer membrane in apoptosis. *EMBO J.* 35, 402–413
45. Sohnel, A.C. et al. (2016) Probing of protein localization and shuttling in mitochondrial microcompartments by FLIM with sub-diffraction resolution. *Biochim. Biophys. Acta* 1857, 1290–1299
46. Blacker, T.S. et al. (2014) Separating NADH and NADPH fluorescence in live cells and tissues using FLIM. *Nat. Commun.* 5, 3936
47. Sugiura, A. et al. (2017) Newly born peroxisomes are a hybrid of mitochondrial and ER-derived peroxisomes. *Nature* 542, 251–254
48. Zhou, Q. et al. (2016) Mitochondrial endonuclease G mediates breakdown of paternal mitochondria upon fertilization. *Science* 353, 394–399
49. Shu, X. et al. (2011) A genetically encoded tag for correlated light and electron microscopy of intact cells, tissues, and organisms. *PLoS Biol.* 9, e1001041
50. Lam, S.S. et al. (2015) Directed evolution of APEX2 for electron microscopy and proximity labeling. *Nat. Methods* 12, 51–54
51. Martell, J.D. et al. (2012) Engineered ascorbate peroxidase as a genetically encoded reporter for electron microscopy. *Nat. Biotechnol.* 30, 1143–1148
52. Ariotti, N. et al. (2018) Ultrastructural localisation of protein interactions using conditionally stable nanobodies. *PLoS Biol.* 16, e2005473
53. Valm, A.M. et al. (2017) Applying systems-level spectral imaging and analysis to reveal the organelle interactome. *Nature* 546, 162–167
54. Gatta, A.T. and Levine, T.P. (2017) Piecing together the patchwork of contact sites. *Trends Cell Biol.* 27, 214–229
55. Helmstaedter, M. et al. (2013) Connectomic reconstruction of the inner plexiform layer in the mouse retina. *Nature* 500, 168–174
56. Helmstaedter, M. (2013) Cellular-resolution connectomics: challenges of dense neural circuit reconstruction. *Nat. Methods* 10, 501–507
57. Beier, T. et al. (2017) Multicut brings automated neurite segmentation closer to human performance. *Nat. Methods* 14, 101–102
58. Haberl, M.G. et al. (2018) CDeep3M—Plug-and-Play cloud-based deep learning for image segmentation. *Nat. Methods* 15, 677
59. de Jonge, N. and Peckys, D.B. (2016) Live cell electron microscopy is probably impossible. *ACS Nano* 10, 9061–9063
60. Combs, C.A. and Shroff, H. (2017) Fluorescence microscopy: a concise guide to current imaging methods. *Curr. Protoc. Neurosci.* 79, 2.1.1–2.1.25.
61. Imamura, H. et al. (2009) Visualization of ATP levels inside single living cells with fluorescence resonance energy transfer-based genetically encoded indicators. *Proc. Natl. Acad. Sci. U S A* 106, 15651–15656
62. Tang, J.L. et al. (2014) A ratiometric fluorescent probe with unexpected high selectivity for ATP and its application in cell imaging. *Chem. Commun. (Camb)* 50, 15411–15414
63. Tantama, M. et al. (2013) Imaging energy status in live cells with a fluorescent biosensor of the intracellular ATP-to-ADP ratio. *Nat. Commun.* 4, 2550
64. Depaoli, M.R. et al. (2018) Real-time imaging of mitochondrial ATP dynamics reveals the metabolic setting of single cells. *Cell Rep.* 25, 501–512
65. Rothstein, E.C. et al. (2005) Skeletal muscle NAD(P)H two-photon fluorescence microscopy in vivo: topology and optical inner filters. *Biophys. J.* 88, 2165–2176
66. Sukumar, M. et al. (2016) Mitochondrial membrane potential identifies cells with enhanced stemness for cellular therapy. *Cell Metab.* 23, 63–76
67. San Martin, A. et al. (2014) Imaging mitochondrial flux in single cells with a FRET sensor for pyruvate. *PLoS One* 9, e85780
68. Balaban, R.S. et al. (1986) Relation between work and phosphate metabolite in the in vivo paced mammalian heart. *Science* 232, 1121–1123
69. Chance, B. et al. (1981) Mitochondrial regulation of phosphocreatine/inorganic phosphate ratios in exercising human muscle: a gated ³¹P NMR study. *Proc. Natl. Acad. Sci. U S A* 78, 6714–6718
70. Wilson, J.R. et al. (1985) Evaluation of energy metabolism in skeletal muscle of patients with heart failure with gated phosphorus-31 nuclear magnetic resonance. *Circulation* 71, 57–62
71. Penjweini, R. et al. (2018) Intracellular oxygen mapping using a myoglobin-mCherry probe with fluorescence lifetime imaging. *J. Biomed. Opt.* 23, 1–14
72. Esipova, T.V. et al. (2019) Oxyphor 2P: a high-performance probe for deep-tissue longitudinal oxygen imaging. *Cell Metab.* 29, 736–744
73. Willingham, T.B. et al. (2019) mitoRACE: evaluating mitochondrial function in vivo and in single cells with subcellular resolution using multiphoton NADH autofluorescence. *J. Physiol.* Published online September 6, 2019. <https://doi.org/10.1113/JP278611>
74. Chen, T.T. et al. (2015) Fluorescence activation imaging of cytochrome c released from mitochondria using aptameric nanosensor. *J. Am. Chem. Soc.* 137, 982–989
75. Zhang, J. et al. (2019) Surface-enhanced Raman scattering-fluorescence dual-mode nanosensors for quantitative detection of cytochrome c in living cells. *Anal. Chem.* 91, 6600–6607
76. Liu, Y. et al. (2016) Upconversion nano-photosensitizer targeting into mitochondria for cancer apoptosis induction and cyt c fluorescence monitoring. *Nano Res.* 9, 3257–3266
77. Ma, L. et al. (2017) A novel upconversion@polydopamine core@ shell nanoparticle based aptameric biosensor for biosensing and imaging of cytochrome c inside living cells. *Biosens. Bioelectron.* 87, 638–645
78. Zhang, H. et al. (2018) Label-free fluorescence imaging of cytochrome c in living systems and anti-cancer drug screening with nitrogen doped carbon quantum dots. *Nanoscale* 10, 5342–5349
79. Cai, M. et al. (2019) Label-free fluorometric assay for cytochrome c in apoptotic cells based on near infrared Ag₂S quantum dots. *Anal. Chim. Acta* 1056, 153–160
80. Shamsipur, M. et al. (2016) Detection of early stage apoptotic cells based on label-free cytochrome c assay using bioconjugated metal nanoclusters as fluorescent probes. *Anal. Chem.* 88, 2188–2197
81. Tang, J. et al. (2018) Azoreductase and target simultaneously activated fluorescent monitoring for cytochrome c release under hypoxia. *Anal. Chem.* 90, 5865–5872
82. Qi, G. et al. (2018) Smart plasmonic nanorobot for real-time monitoring cytochrome c release and cell acidification in apoptosis during electrostimulation. *Anal. Chem.* 91, 1408–1415

83. Smith, N.A. et al. (2018) Fluorescent Ca²⁺ indicators directly inhibit the Na, K-ATPase and disrupt cellular functions. *Sci. Signal.* 11, eaal2039
84. Lock, J.T. et al. (2015) A comparison of fluorescent Ca²⁺ indicators for imaging local Ca²⁺ signals in cultured cells. *Cell Calcium* 58, 638–648
85. Akerboom, J. et al. (2013) Genetically encoded calcium indicators for multi-color neural activity imaging and combination with optogenetics. *Front. Mol. Neurosci.* 6, 2
86. Davidson, S.M. and Duchen, M.R. (2018) Imaging mitochondrial calcium fluxes with fluorescent probes and single- or two-photon confocal microscopy. In *Mitochondrial Bioenergetics* (Palmeira, C.M. and Moreno, A.J. eds), pp. 171–186, Springer
87. Whitaker, M. (2010) Genetically encoded probes for measurement of intracellular calcium. *Methods Cell* 99, 153–182
88. De Michele, R. et al. (2014) Mitochondrial biosensors. *Int. J. Biochem. Cell Biol.* 48, 39–44
89. Wu, J. et al. (2014) Red fluorescent genetically encoded Ca²⁺ indicators for use in mitochondria and endoplasmic reticulum. *Biochem. J.* 464, 13–22
90. Contreras, L. et al. (2010) Mitochondria: the calcium connection. *Biochim. Biophys. Acta* 1797, 607–618
91. Pozzan, T. and Rudolf, R. (2009) Measurements of mitochondrial calcium in vivo. *Biochim. Biophys. Acta* 1787, 1317–1323
92. Zhang, X. and Gao, F. (2015) Imaging mitochondrial reactive oxygen species with fluorescent probes: current applications and challenges. *Free Radic. Res.* 49, 374–382
93. Dikalov, S.I. and Harrison, D.G. (2014) Methods for detection of mitochondrial and cellular reactive oxygen species. *Antioxid. Redox Signal.* 20, 372–382
94. Woolley, J. et al. (2013) Recent advances in reactive oxygen species measurement in biological systems. *Trends Biochem. Sci.* 38, 556–565
95. Wang, X. et al. (2013) Imaging ROS signaling in cells and animals. *J. Mol. Med.* 91, 917–927
96. Sieprath, T. et al. (2016) Integrated high-content quantification of intracellular ROS levels and mitochondrial morphofunction. In *Focus on Bio-Image Informatics* (De Vos, W.H. et al. eds), pp. 149–177, Springer
97. Glancy, B. et al. (2015) Mitochondrial reticulum for cellular energy distribution in muscle. *Nature* 523, 617–620
98. Picard, M. et al. (2015) Trans-mitochondrial coordination of cristae at regulated membrane junctions. *Nat. Commun.* 6, 6259
99. Vincent, A.E. et al. (2017) Mitochondrial nanotunnels. *Trends Cell Biol.* 27, 787–799
100. Patel, K.D. et al. (2016) The electrochemical transmission in I-Band segments of the mitochondrial reticulum. *Biochim. Biophys. Acta* 1857, 1284–1289
101. Glancy, B. et al. (2017) Power grid protection of the muscle mitochondrial reticulum. *Cell Rep.* 19, 487–496
102. Santo-Domingo, J. et al. (2013) OPA1 promotes pH flashes that spread between contiguous mitochondria without matrix protein exchange. *EMBO J.* 32, 1927–1940
103. Poburko, D. et al. (2011) Dynamic regulation of the mitochondrial proton gradient during cytosolic calcium elevations. *J. Biol. Chem.* 286, 11672–11684
104. Belousov, V.V. et al. (2006) Genetically encoded fluorescent indicator for intracellular hydrogen peroxide. *Nat. Methods* 3, 281–286
105. McWilliams, T.G. et al. (2016) mito-QC illuminates mitophagy and mitochondrial architecture in vivo. *J. Cell Biol.* 214, 333–345
106. Sun, N. et al. (2015) Measuring in vivo mitophagy. *Mol. Cell* 60, 685–696
107. McWilliams, T.G. et al. (2018) Basal mitophagy occurs independently of PINK1 in mouse tissues of high metabolic demand. *Cell Metab.* 27, 439–449
108. Szabadkai, G. et al. (2004) Drp-1-dependent division of the mitochondrial network blocks intraorganellar Ca²⁺ waves and protects against Ca²⁺-mediated apoptosis. *Mol. Cell* 16, 59–68
109. Molina, A.J. et al. (2009) Mitochondrial networking protects beta-cells from nutrient-induced apoptosis. *Diabetes* 58, 2303–2315
110. Bleazard, W. et al. (1999) The dynamin-related GTPase Dnm1 regulates mitochondrial fission in yeast. *Nat. Cell Biol.* 1, 298–304
111. Cieri, D. et al. (2018) SPLICS: a split green fluorescent protein-based contact site sensor for narrow and wide heterotypic organelle juxtaposition. *Cell Death Differ.* 25, 1131–1145
112. Zhang, F. et al. (2015) The cAMP phosphodiesterase Prune localizes to the mitochondrial matrix and promotes mtDNA replication by stabilizing TFAM. *EMBO Rep.* 16, 520–527
113. Ruan, L. et al. (2017) Cytosolic proteostasis through importing of misfolded proteins into mitochondria. *Nature* 543, 443–446
114. Mahajan, N.P. et al. (1998) Bcl-2 and Bax interactions in mitochondria probed with green fluorescent protein and fluorescence resonance energy transfer. *Nat. Biotechnol.* 16, 547–552
115. Sekar, R.B. and Periasamy, A. (2003) Fluorescence resonance energy transfer (FRET) microscopy imaging of live cell protein localizations. *J. Cell Biol.* 160, 629–633
116. Misawa, T. et al. (2013) Microtubule-driven spatial arrangement of mitochondria promotes activation of the NLRP3 inflammasome. *Nat. Immunol.* 14, 454–460
117. Glancy, B. et al. (2014) In vivo microscopy reveals extensive embedding of capillaries within the sarcolemma of skeletal muscle fibers. *Microcirculation* 21, 131–147
118. Zhao, Y. et al. (2011) Genetically encoded fluorescent sensors for intracellular NADH detection. *Cell Metab.* 14, 555–566
119. Hu, H. et al. (2018) Glucose monitoring in living cells with single fluorescent protein-based sensors. *RSC Adv.* 8, 2485–2489
120. Zhao, Y. et al. (2015) SoNar, a highly responsive NAD⁺/NADH sensor, allows high-throughput metabolic screening of anti-tumor agents. *Cell Metab.* 21, 777–789
121. Nicholls, D.G. (2006) Simultaneous monitoring of ionophore- and inhibitor-mediated plasma and mitochondrial membrane potential changes in cultured neurons. *J. Biol. Chem.* 281, 14864–14874